ELSEVIER

Journal of Nuclear Materials 290–293 (2001) 1155–1159

journal of nuclear materials

www.elsevier.nl/locate/jnucmat

RF wall conditioning – a new technique for future large superconducting tokamak

J.K. Xie [*], Y.P. Zhao, J. Li, B.N. Wan, X.Z. Gong, J.S. Hu, X. Gao, X.M. Gu, S.D. Zhang, X.M. Wang, Y.Z. Mao, X.K. Yang, M. Zhen, S.Y. Zhang, HT-7 team

Institute of Plasma Physics, Academia Sinica, Chinese Academy of Science, P.O. Box 1126, Anhui, 230031 Hefei, People's Republic of China

Abstract

A new technique for wall conditioning with a high toroidal magnetic field has been developed on HT-7 superconducting tokamak by launching ion cyclotron resonant wave (ICRF) into plasmas. The RF wall conditioning techniques include hydrogen removal, isotopic and impurity control, boronization and siliconization, which have been proved to be very effective and could be routinely used in daily experiments. © 2001 Elsevier Science B.V. All rights reserved.

Keywords: Wall conditioning; RF discharge

1. Introduction

Wall conditioning is very important to get high plasma performance. Due to the presence of high toroidal magnetic field in superconducting devices, the common wall conditioning techniques, such as DC glow discharge cleaning (GDC) and Taylor discharge cleaning (TDC) could not be used conveniently. A new technique based on RF plasma for wall conditioning has been developed on TORE SUPRA, TEXTOR-94 and HT-7 superconducting tokamaks by injecting ion cyclotron resonant frequency (ICRF) wave into plasmas [1–4].

The theory of plasma production in tokamak by RF power in the ICRF range has been investigated by some authors [5,6]. To initiate the discharge, an RF electric field $E_{\parallel}$ parallel to the magnetic field lines is required. To get higher ionization ratio, the harmonic resonance absorption layers should be inside the discharge chamber. The RF antenna used for plasma heating in HT-7 is suitable for $E_{\parallel}$ generation and plasma production. The RF conditioning technique developed on HT-7 tokamak includes hydrogen removal, impurity cleaning, recycling control, boronization and siliconization. This special technique is a candidate for the wall conditioning of the future large superconducting tokamaks, such as ITER with presence of the high magnetic field.

2. Experimental setup

HT-7 is a medium-sized superconducting tokamak. The machine is normally operated with $I_P = 150$ KA, $B_T = 2$ T, $a = 28.5$ cm, line averaged density $n_e = 1\text{–}5 \times 10^{19}$ m^{-3}, $T_e = 1.0$ keV, $T_i = 0.5$ keV, and a molybdenum limiter configuration. Plasma discharge lasts about 3–5 s. A stainless steel liner is installed with the radius of 0.32 m as the first wall. The ICRF system can be operated under pulsed mode or CW mode. The hardware setup for the RF conditioning is the same as ICRF heating. Three kinds of RF antenna configurations are tested. A 1/4-turn antenna with Faraday shielding is installed at low field side of torus. A 1/2 turn long antenna is at the high field side. And an ion Bernstein wave (IBW) antenna is set in the midplane at low field side. The arrangement of whole system is shown as Fig. 1.

---

[*] Corresponding author. Tel.: +86-551 559 1310; fax: +86-551 559 1310.

E-mail address: jkxie@mail.ipp.ac.en (J.K. Xie).

PII: S0022-3115(00)00495-5

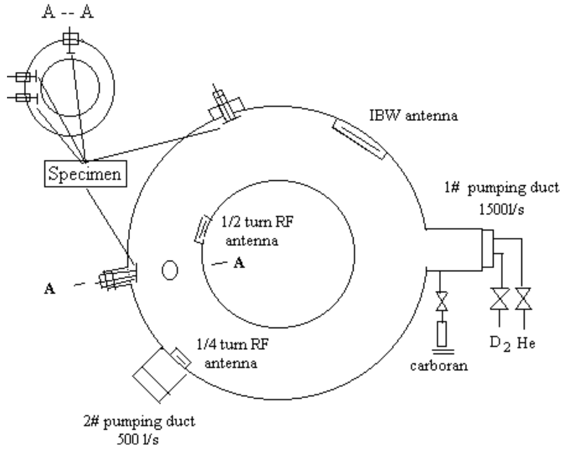

Fig. 1. The setup of RF conditioning system on HT-7 tokamak.

Conditioning procedure using different antennas were compared. The low field side antenna produces plasma mainly concentrated in a limited area close to the midplane. The ion Bernstain wave antenna produces plasma located at the outer part of the chamber. The high field side long antenna plays the best. It produces homogeneous plasma spread over the whole chamber. So in most cases in the following results, that antenna was used.

For a wide range of toroidal field, RF plasma can be easily produced by injecting ICRF power of 5–50 kw in both helium and deuterium gases. Parameter scan have been conducted on toroidal field (0.1–2.5 T), gas pressure (8×10^{-4}–5×10^{-1} Pa) and radio frequency (RF) (24–30 MHz) to optimize the cleaning efficiency. The basic RF plasma parameters produced by different antenna configurations are measured by several diagnostics. Quadropole mass spectrometer (QMS) analysis during and after RF conditioning is carried out. Electron temperature is deduced from visible line spectrum and ECE measurement. Electron density is measured by HCN interferometer and Langmuir probes. And ion temperature is measured by neutral particle analyzer (NPA). Normally the parameters of the plasma for conditioning are as follows: T_e in the range of 3–10 eV with RF power of 35 kW, (the electron temperature of helium RF plasma is two times high as deuterium plasma with same discharge condition), density in the range of 0.5–3×10^{17} m^{-3}, and ion temperature about 1–2 keV with high-energy tail of a few tens keV.

3. Particle removal

Two effects governing the conditioning efficiency are outgassing rate of impurities from the wall and the ionization rate of desorbed molecules which induce a redeposition. The optimization was made on increasing the conditioning efficiency and minimizing the hydrogen re-ionization and re-deposition probability. Practically a pulsed RF mode was used to prevent the overheat of RF feedthrough. The best pulsed mode is with RF power 0.3 s on and 1.5 s off with gas pressure higher than 1×10^{-2} Pa, while electron density is high and temperature is low (<5 eV). The RF injection power level also plays a very important role for higher hydrogen and impurity removal efficiency. But the efficiency is independent on injected RF frequency (24–30 MHz) and weakly relates to toroidal field. The optimized RF power level is lower than 20 kW. Normally helium RF discharge is used for particle removing, for example, replacement of hydrogen (or its isotopes). That makes plasma start up relatively easier and the particle recycling in a controlled manner. Deuterium ICRF discharge could be used for surface cleaning and wall isotope control. The optimized filling pressure is 1×10^{-1} Pa. The electron temperature is (2–3 eV), lower than helium discharge.

Fig. 2 shows the particle removal rate against conditioning time. The RF power is 5 kW and filling pressure 2×10^{-2} Pa. The quantity of removed hydrogen is proportional to the conditioning time, while CO and H_2O (mass number 28 and 18) become slow after 120 min and gradually saturate after 160 min. Fig. 3 shows the QMS data results before ICRF wall conditioning and after 60 min pulsed 15 KW RF discharge followed by 30 min pumping. After ICRF wall conditioning, CO reduced by a factor of three and H_2O reduced more than two times. For comparison between GDC and RF conditioning, the experimental data in past 3 years are also shown. The particle-removing rates of RF cleaning to H_2, H_2O and CO are about 20, 120 and 560 times higher than those obtained by GDC, respectively.

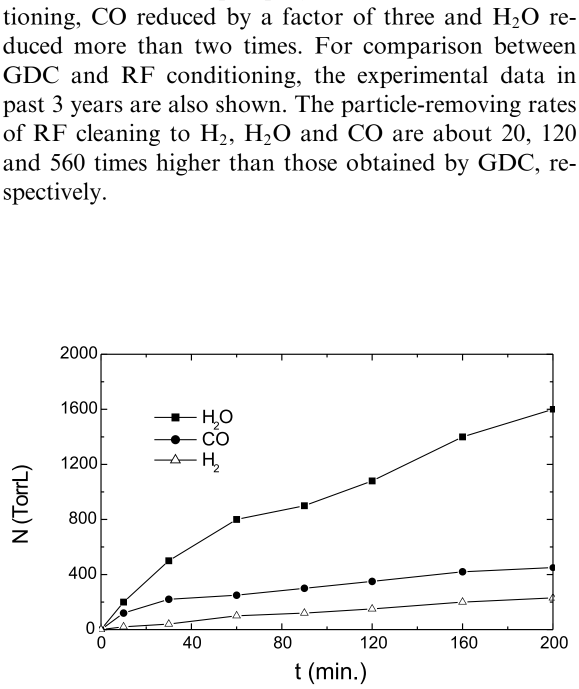

Fig. 2. Particle removing versus cleaning time.

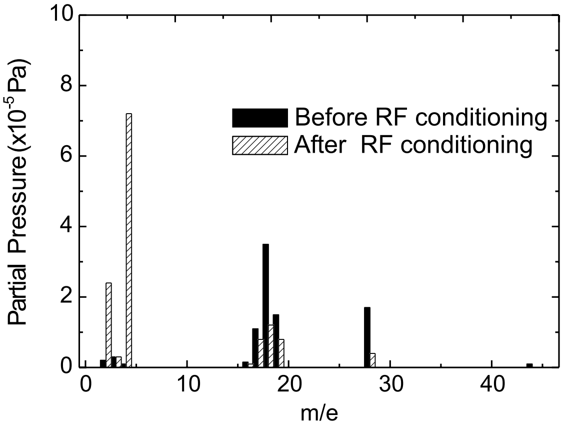

Fig. 3. QMS data before and after ICRF wall conditioning. $B_T = 1.5$ T, $f = 30$ MHz, Pv = 0.15 Pa.

4. Boronization

From the experiences of boronization on other tokamaks [7,8], non-toxic and non-explosive solid substance carborane ($C_2B_{10}H_{12}$) was chosen as the boronization material in HT-7 tokamak for safe handling and exhausting. The plasma facing liner was baked to 150–200°C and the vacuum vessel wall about 100°C. The toroidal magnetic field was about 1.8 T and the RF frequency was 30 MHz. With these parameters, the fundamental resonance layer of ICRF hydrogen was located inside the plasma region.

In order to get higher adhesion of the film, 60-min helium RF pre-conditioning was carried out. The pulsed RF plasma was initiated with the filling pressure 5×10^{-3} Pa and gradually increased up to 0.3 Pa. The carborane was kept in a stainless steel container close to the gas injection inlet and connected to the first pumping duct shown in Fig. 1. Twelve samples of different material specimens (graphite, stainless steel) were placed round the radius of the liner. When boronization started, the carborane container was heated to 60°C and partial pressure of 0.2 Pa was kept. During boronization helium carborane ratio was reduced to 1/1. Plasma color gradually changed from light green to pink, which indicated the injection of carborane vapor. Since several different species of particle existed in the plasma, their harmonic cyclotron resonant layers were clearly observed from the RF plasma. The boronization process lasted for 90 min with 4 g of carborane evaporation. After that, 30 min helium cleaning discharge was applied to remove the huge hydrogen absorption during boronization with reduced RF power to 3 kW to prevent heavy bombardment on the fresh film.

QMS analysis was done right after the helium RF discharge. The main residential gases were H_2, HD, He and D_2. Fig. 4 gives the comparison of partial pressures before and after RF boronization. It shows a substantial reduction of water vapor and 40% reduction of CO. The film properties of samples were analyzed by X-ray induced photoelectron spectroscopy (XPS). Some of the samples were taken out after boronization and others remained through out experiment. XPS showed a fine amorphous boron–carbon film (a-C/B:H). Boron had a well-defined composition, which was homogeneous in depth, as could be seen from the depth profile of graphite specimen shown in Fig. 5. B/C ratio was about 3 up to 220 nm depth. The oxygen concentration was about 10% from the presence of H_2O and CO during the film deposition.

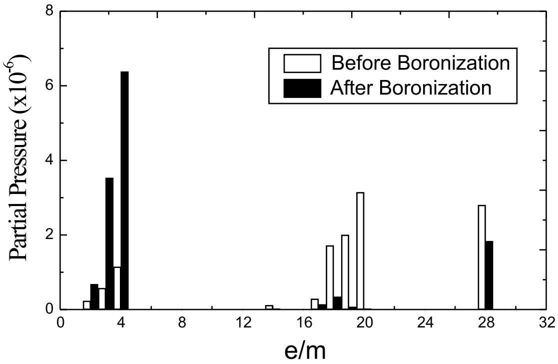

Fig. 4. Comparison of QMS data before and after RF boronization coating, $B_T = 1.5$ T, $f = 30$ MHz, $P_{RF} = 10$ kW, Pv = 0.3 Pa.

The strong oxygen gettering ability was observed when the film was exposed to the bombardment of plasma discharge shown in Fig. 5(b). Oxygen content increased from 10% to 25% and boron content decreased from 60% to 50% after 250 shots. Quantitative analysis of composition of oxygen, boron and carbon showed

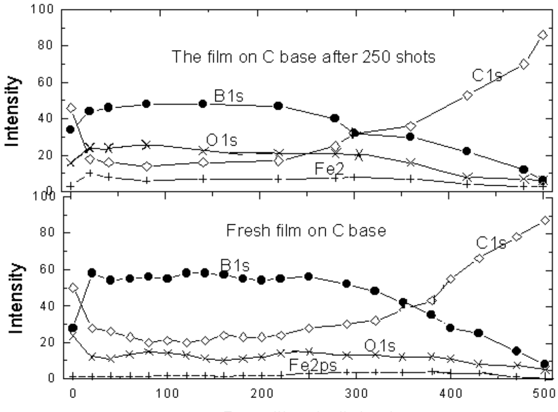

Fig. 5. XPS analysis for the boronized graphite specimen before and after 250 plasma discharges.

that B_2O_3 (192 eV) exists in the film, especially in the bombarded film. In the fresh film, boron appeared in the forms of B–B, B–C and B–O bonds. While carbon dwelled in the forms of C–C and C–B bonds. With the bombardment of particles, the C–O bond also formed in the film. The CO came from the porous structure of the film. This was the main reason of high content of mass number 28, which is shown in Fig. 4. The film thickness had reduced to about 80 nm after 250 shots. Generally speaking, the lifetime of 4 g film lasted for about 1500 shots.

Films were poloidally non-uniform by the low field side antenna because of the anisotropy of RF discharge during boronization, as could be seen from the non-uniform distribution of ion cyclotron resonant layers. The film thickness along the poloidal direction was different. More uniform films were produced by high field side long antenna, while the plasma was nearly homogeneous along both toroidal and poloidal directions.

The plasma performance was immediately improved after RF boronization. The metal impurity lines disappeared. The visible lines of carbon and oxygen reduced by a factor of 3. The radiation power significantly dropped from 80% of input power to the level of 16%. The Z_{eff} dropped close to unity at the density 5×10^{19} m^{-3}. Wider Hugill stability operation region was obtained. Hence higher LHW current drive and ICRF heating efficiency were achieved. Longer plasma shot up to 10 s was easy to achieve.

The RF discharge in bronzed wall was also used to control the ratio of H/(H+D) for ICRF minority heating. Even when the ratio was as high as 60%, two periods of 30 min D_2 RF discharge could make it drop to 15%.

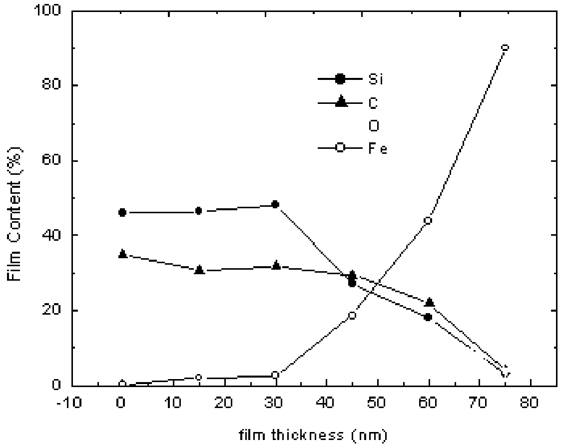

Fig. 6. XPA analysis for Si film on SS specimen.

5. Siliconization

Siliconization was carried out by using high-field side long RF antenna too. Two conditions with different SiH_4 to He ratio were tested for optimization. In the first condition, ratio of SiH_4 to He was about 5/95 at the filling pressure range of $Pv = 8 \times 10^{-3}$ Pa. Pulsed mode was used with one-second on and one-second off. The RF power was about 10 kW and the pre-cleaning was not necessary. The whole procedure usually lasted for 30–60 min. Plasma discharge was fired right after siliconization and good plasma discharges were obtained. But the silicon film effected less than 100 shots. The XPS analysis showed that the film property was not as good as it was in TEXTOR [8–10], such as thickness, uniformity and silicon contents. In second condition, higher ratio of SiH_4 to He (10/90), higher RF power (15 kW) and filling pressure (0.06–0.1 Pa) were used. The film property was better. Fig. 6 shows the XPS analysis results of silicon film on the SS specimen. A fine uniform silicon film was produced, mainly in the form of SiC and Si. Deposition rate was about 1 nm/min. As the SS specimen samples were set in the position of 1 cm behind the liner and without heating capacity, the film properties of the first wall should be better than those on the specimen's. Even after 400 standard shots, the effects of siliconization still remained. By chance, after an air leak, RF siliconization could quickly recover the discharge. The whole treatment took only 1 h. Z_{eff} again dropped below 3, and plasma performance returned to a good state.

Usually the density control was easy after siliconization without need of successive RF processing. The uniformity of the film was as good as boron one. The difference for the film thickness at the different poloidal and toroidal directions was within 20%. But the lifetime is much shorter than boronization. That might be because that the thickness of the film was only about

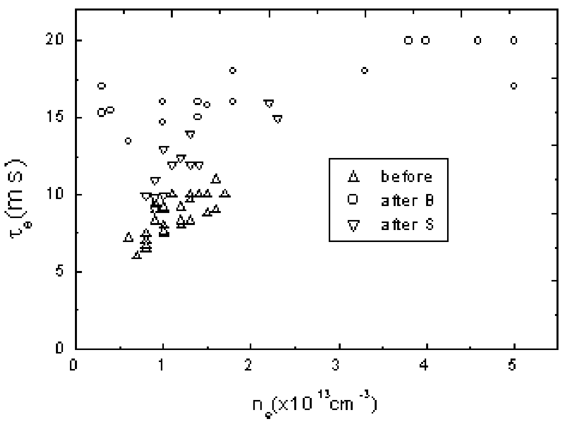

Fig. 7. Comparison of energy confinement time after the different wall coating.

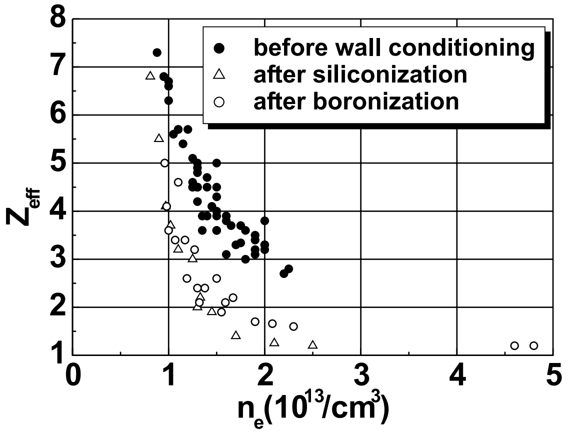

Fig. 8. Comparison of impurity content after the different wall coating.

60 nm. The main reason for much thinner silicon film was due to the high ratio of helium to silane gas. Higher silage content in the working gas would benefit the higher film thickness but difficult for handling.

Both RF siliconization and boronization could significantly improve the plasma performance. Plasma performance improved right after siliconization procedure. Compared to boronization, Lower *q* and wider stable operation region were achieved. Higher electron temperature was obtained. Fig. 7 shows the energy confinement time of ohmic discharges in different wall conditioning techniques.

Maximum increase achieved energy confinement time 50% after siliconization and increased by a factor of 2 after boronization. Slightly hollow and wider density and electron temperature profiles were formed after siliconization. The sawteeth reverse radius changed from 4 to 9 cm. The edge safety factor could be as low as 2.45. The impurities and radiation loss were reduced. A quantitative comparison of impurity reduction via density is shown as in Fig. 8. The main impurities (carbon and oxygen) were reduced by a factor of 2. Z_{eff} dropped significantly after RF siliconization and boronization. The boron film lasted longer than the silicon one simply because of its higher thickness.

6. Summary

RF wall techniques has been tested, developed and routinely used in HT-7 tokamak. This technique is suitable for future large superconducting devices in the presence of continuous high magnetic fields. The particle-removing rate and cleaning efficiency are much higher than those obtained by GDC technique. Basic plasma parameters produced by different antenna configuration and their role to get best cleaning and coating effects have been studied. High field side long antenna and pulsed mode have shown good results. The B/C:H and Si/C:H films have also shown higher adhesion, better uniformity and longer lifetime in plasma discharges than those obtained by normal GDC method. Plasma performance has been improved after RF boronization and siliconization. Higher LHW current driven and ICRF heating efficiency were obtained. Long pulse discharges up to 10 s have been achieved.

References

[1] E. Gauthier et al., J. Nucl. Mater. 241–243 (1997) 553.
[2] E. De La Cal, E. Gauthier, Plasma Phys. Contol. Fus. 39 (1997) 1083.
[3] Y.P. Zhao, Chin. Phys. Lett. 14 (1997) 916.
[4] J. Li et al., Nucl. Fus. 39 (1999) 973.
[5] A.I. Lyssoivan et al., Nucl. Fus. 32 (1992) 1361.
[6] M.D. Carter et al., Nucl. Fus. 30 (1990) 723.
[7] M. Yamage et al., Jpn. J. Appl. Phys. 32 (1993) 3968.
[8] J. Winter et al., Phys. Rev. Lett. 71 (1993) 1549.
[9] J. von Seggern et al., J. Nucl. Mater. 220–222 (1995) 677.
[10] U. Samm et al., J. Nucl. Mater. 220–222 (1995) 25.